JOURNAL OF APPLIED ELECTROCHEMISTRY **10** (1980) 757–763

The Li/TiS_2 cell with LiSCN electrolyte

B. M. L. RAO, D. J. EUSTACE, J. A. SHROPSHIRE

Advanced Energy Systems Laboratory, Corporate Research–Technology Feasibility Center, Exxon Research and Engineering Company, PO Box 45, Linden, New Jersey 07036, USA

Received 9 January 1980

An ambient temperature, rechargeable lithium/titanium disulphide cell with a lithium thiocyanate–1,3-dioxolane (DOL)–1,2-dimethoxyethane (DME) organic electrolyte was investigated. Electrolyte compositions of 2.5–3.5 molal LiSCN in solvent compositions from 100% DOL to 0.80:0.20::DOL:DME were tested. NMR, infrared spectroscopy and linear-sweep voltammetric studies indicated that the electrolyte was thermally and electrochemically stable, except for the slow formation of dioxolane oligomers. Test cells contained 10–30 mA h cm^{-2} of TiS_2 with two- to sixfold excess of Li in parallel-plate, prismatic configuration. Performance delivered 80–90% of theoretical charge on first discharge and showed not only a rate-dependent cycle life, but also sensitivities to the (anode loading)/(cathode loading) ratio and cathode charge density. Cells with 10–15 mA h cm^{-2} of TiS_2 and four- to sixfold excess Li operated 35–50 cycles at $C/5$ to $C/15$ rates, while 30 mA h cm^{-2} cathodes with 3:1::anode:cathode ratio cycled 10–20 cycles at $C/10$. Results of half-cell studies, performance variation with temperature and overcharge and overdischarge behaviour of the cells are presented. Possible causes of the loss of efficiency during cycling are discussed.

1. Introduction

During the past 10 years, considerable experience has been gathered on the capabilities of a number of commercial lithium, organic electrolyte primary cells. These include Li/V_2O_5, $Li/AgCrO_4$, Li/CuO, $Li/CuCl_2$, Li/CF_x, Li/FeS, Li/MnO_2, Li/SO_2, and $Li/SOCl_2$ systems. In general, the lithium cells have demonstrated higher energy density and lower self-discharge rate under elevated temperature storage and better low temperature performance than zinc-based aqueous primary cells.

Attempts to develop ambient temperature rechargeable cells with organic electrolytes have not been as successful. The lack of 100% reversibility for the electroplating and stripping of lithium, attended by dendritic electrodeposition of the active material, has been one of the bottlenecks in operating the negative electrode. A high overpotential for charge–discharge (nickel halides) and the cathode salt solubility (silver and copper halides) have been major problems at the positive electrode. The severity of the lithium electrode problem has been minimized either by using alloy electrodes [1], or by rendering the cell cathode-limiting in capacity with excess lithium to compensate for the loss of efficiency. A new approach to the positive electrode problem was provided by the use of intercalation compounds (transition metal chalcogenides) instead of the transition metal halide salts [2]. In this context, a ~ 5 hour-rate, ambient temperature Li/TiS_2 rechargeable cell, with an operating life of > 250 deep-discharge cycles, with 3.0 M $LiClO_4$–dioxolane, was reported earlier from our laboratory [3]. Due to a safety problem, i.e., an explosive hazard associated with the perchlorate anion in the ether medium, further development was delayed in favour of exploring alternative, safe electrolytes, including a series of lithium organometallic salt systems [4]. Successful operation of rechargeable Li/TiS_2 cells with $LiAsF_6$–2-methyltetrahydrofuran has been reported recently by Holleck *et al.* [5]. This paper deals with Li/TiS_2 cells with a LiSCN–1,3-dioxolane (DOL)–1,2-dimethoxyethane (DME) electrolyte.

The preparation of anhydrous LiSCN has been reported by Lee [6] and Saar *et al.* [7]. Mention has been made of the use of LiSCN in 2- and 2,5-alkylated tetrahydrofurans [8], 2- and 2,6-alkylated

0021–891X/80/060757–07$02.70/0

pyrans [8], 3-methyl-2-oxazolidone and tetrahydrofuran-dimethoxyethane [9] and dioxolane [10–12] as lithium battery electrolytes. No information on the operation of rechargeable Li/TiS_2 cells with LiSCN–DOL–DME has been presented in the published literature.

2. Experiments and results

2.1. *Electrolyte investigations*

2.1.1. Solubility and thermal stability. Anhydrous LiSCN is soluble in DOL and DOL–DME mixtures to greater than 4.5 M at room temperature. Freshly prepared LiSCN–DOL electrolytes are clear, colourless liquids stable to freeze–thaw cycles to -55° C. When stored in the dark, at room temperature, or at 50° C, LiSCN–DOL solutions and LiSCN–DOL–DME solutions acquire a light yellow colour, attended by precipitation of small amounts of solids. Electrolytes stored for one month at 50° C exhibit a $3\frac{1}{2}$-fold increase in viscosity, with about a 10% increase in specific resistance. These results, coupled with the observed signal broadening of DOL protons in NMR studies and the generation of absorptions at 890 cm^{-1} and 1010 cm^{-1} in i.r. spectra of aged solutions, indicate the formation of poly-DOL oligomers [13]. The water content of the electrolytes was < 200 ppm.

2.1.2. Specific resistance of LiSCN electrolytes. The composition–specific resistance profile shows a plateau minimum in LiSCN–DOL, where LiSCN is greater than 2.0 M. Similarly, LiSCN–DOL–DME shows a minimum at compositions in which LiSCN is greater than 1.7 M and DME is less than 20 wt% of the solvent. Typical Arrhenius plots of the specific resistance ρ versus 1/temperature for selected compositions are shown in Figs. 1 and 2.

2.1.3. Electrochemical stability. Linear-sweep voltammetric investigations of LiSCN–DOL and LiSCN–DOL–DME electrolytes were carried out on a tantalum electrode in the potential range -0.1 to $+3.25$ V with a lithium reference and counter-electrode. A background current of 15 $\mu A\,cm^{-2}$ and two peaks, one at 0.0 V (versus Li) and the other at 3.25 V (versus Li), attributable to lithium deposition/dissolution and the redox couple of $(SCN)_2/SCN^-$, were observed at room temperature in both fresh electrolyte and electrolyte aged at 50° C for one month.

There was no visible tarnishing of lithium metal in contact with fresh and 50° C-aged electrolytes or on storage of lithium metal in contact with the electrolyte at 65° C for one month under anhydrous conditions.

2.2. *Li/TiS_2 cell investigations*

2.2.1. Test cell. The Li/TiS_2 cells constructed for test were of one-anode, one-cathode, parallel-plate prismatic configuration. The positive was a sintered porous cake of 90 wt% TiS_2 and 10 wt% polytetrafluoroethylene powder, which was hot-pressed on to a tantalum grid. The negative was 0.051 cm, or 0.025 cm thick, lithium foil loaded on a copper grid. The electrode areas were 6.45 cm^2. They were individually enclosed in heat-sealed, microporous polypropylene bags, and were sandwiched as parallel-plates across a 0.04 cm porous fibreglass mat separator. A polyethylene bag with the top side open, into which the electrode arrangement was placed and clamped, served as the cell container. The cells were

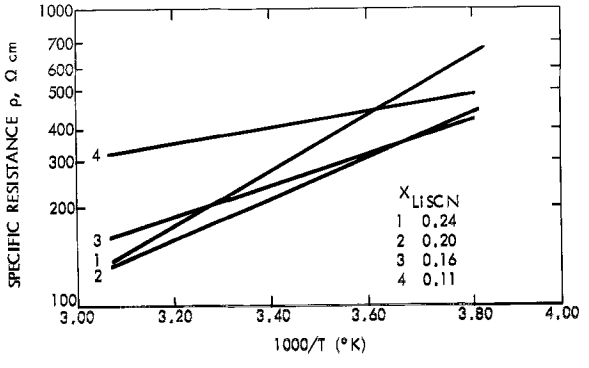

Fig. 1. Specific resistance versus 1/temperature profiles for LiSCN–DOL electrolytes.

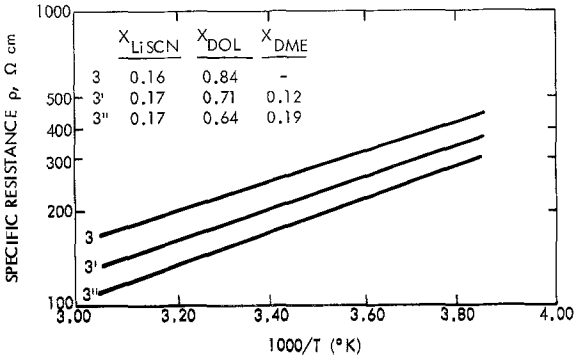

Fig. 2. Specific resistance versus 1/temperature profiles for LiSCN–DOL–DME electrolytes.

assembled in the dry room (< 1.5% RH) and completed by placement in suitable sealed glass jars with electrical leads to exclude atmospheric contamination. The cells were tested following addition of 2.5–3.5 M LiSCN–DOL–DME electrolyte and allowing 2–16 h for wetting.

Lithium electrodeposition and stripping experiments, using 2.5 M–3.5 M LiSCN–DOL–DME electrolyte, on a copper substrate at 0.4–1.5 mA cm^{-2} (delivery 5–20 mA cm^{-2}) showed 85–40% efficiency. The results suggested the need for using sufficient excess of lithium to compensate for losses due to inefficiency. This, combined with the ready availability of 0.025 and 0.051 cm lithium foil, prompted the use of 45 and 90 mA h cm^{-2} lithium electrodes in the cells.

The TiS_2 cathode capacity of the test cell was generated from a study of the sensitivity of electrode performance to capacity density. Fig. 3 gives the variation of the TiS_2 utilization efficiency on the first discharge, with electrode loading at a series of current densities, to 1.4 V (versus Li reference). A sharp drop in TiS_2 utilization occurs at ~ 45 mA h cm^{-2} for these test cathodes.

2.2.2. Tests. Preliminary investigations were carried out to assess the cycling capability of Li/TiS_2 cells in terms of the TiS_2 electrode charge density, current density and cut-off potential. These experiments indicated that cells with low charge density (~ 5–10 mA h cm^{-2}), operating at low current density (0.25 mA cm^{-2}) and to shallow depths (~ 10%), would deliver several hundred cycles. Deep-discharge cycling behaviour of 10–30 mA h cm^{-2} TiS_2 electrodes at 0.25–3.1 mA cm^{-2} was extensively studied.

The discharge rate capacity of Li/TiS_2 cells of the configuration and composition discussed above

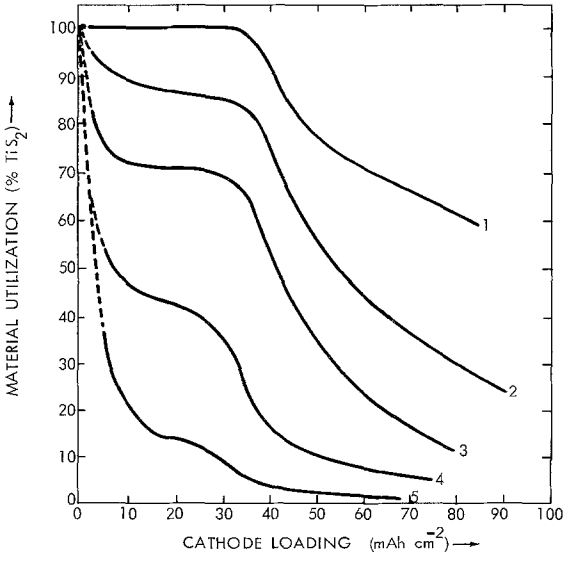

Fig. 3. Variation of TiS_2 utilization with cathode loading in TiS_2 cells (porosity ~ 45%). Electrolyte: 3.4 M LiSCN–DOL–DME (92 W/0:8 W/0); discharge current (in mA cm^{-2}) 1, 0.62; 2, 1.25; 3, 2.5; 4, 5.0; 5, 10.

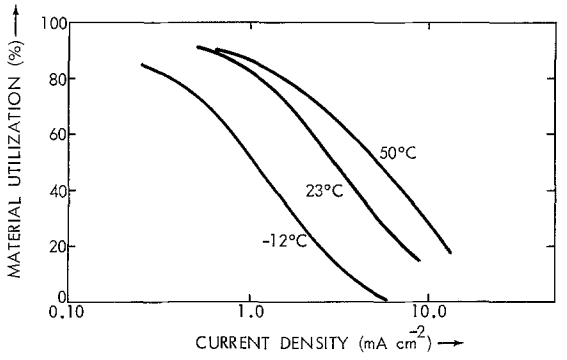

Fig. 4. First-discharge performance of Li/TiS_2 cells with 2.5 M LiSCN–DOL electrolyte.

is presented in Fig. 4. The measurement was carried out in the following constant-current test sequence to 1.4 V cut-off. The cells were first discharged at the highest current, indicated in Fig. 4, and the material utilization (% MU) of TiS_2 was recorded. The cells were then left to stand for a minimum of 15 min on open-circuit to allow 85–90% recovery of the final open-circuit voltage. After the rest period, the cells were discharged at a lower current, typically 25–50% of the previous discharge, and the TiS_2 utilization efficiency was determined. The cumulative TiS_2 utilization to the test current was computed and plotted assuming that the total capacity available at any current is the sum of all the capacities obtained at prior higher current tests. This procedure provided the data in Fig. 4 at various temperatures.

In a similar way to the above, the cycling behaviour of the cells was tested. The cells were discharged at 10–20 mA on the first subset of cycles, with a 1.2–1.6 V cut-off. Subsequent cycling was carried out at $C/10$ to $C/50$ rates. The cells were charged at 5 mA to 2.6 V at constant current, followed by constant potential charging for 10 h to 2.6 V. Table 1 summarizes the cycling behaviour of cells with varying cathode capacities (204–66.9 mA h in^2) and anode loading/cathode loading ratios (2.94–4.48) in their first cycle (columns 2–4) and subsequent cycles (columns 5–9) as the current was decreased. Fig. 5 presents the discharge voltage–time profiles of a typical Li/TiS_2 cell through 50 cycles. It was

Table 1. Li/TiS_2 cell performance

Cathode capacity (mA h)	*Primary discharge*			*Subsequent discharges*				
	Discharge rate (mA)	*Cut-off potential* (V)	*MU* (%)	*Cycle number*	*Cumulative capacity* (mA h)	*Discharge rate* (mA)	*Cut-off potential* (V)	*MU* (%)
600 mA h Li cells								
204	20	1.6	53	27	1286	20	1.4	26
				39	2408	10	1.4	42
				54	3946	5	1.4	39
				60	4604	1.6	1.4	52
186	10	1.4	80	16	1339	10	1.5	31
				36	2992	5	1.5	30
				40	3306	1.6	1.2	53
166	10	1.4	86	35	3303	10	1.4	46
				37	3499	1.6	1.4	60
300 mA h Li cells								
92.9	10	1.4	90	15	777	10	1.4	41
71.3	10	1.4	92	35	1299	10	1.4	39
66.9	10	1.4	96	50	1887	10	1.4	40

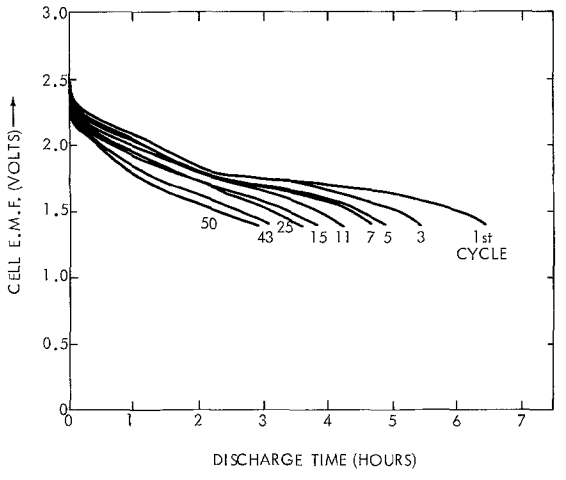

Fig. 5. Cycling behaviour of Li/TiS_2 cells.

discharged at 10 mA to 1.4 V and was charged at 5 mA to 2.6 V at 23° C. The cell was composed of 66.9 mA h TiS_2 and 300 mA h of lithium.

2.2.3. Supplementary investigations. Constant-current, charge (5 mA, 2.8 V)–discharge (10 mA, 1.4 V) experiments were carried out on a TiS_2 half-cell using a lithium reference and a lithium counter-electrode. The coulombic charge balance during cycling was monitored to assess the failure modes of the cells. The details of TiS_2 half-cell behaviour during cycling are shown in Table 2.

The effects of overdischarge and overcharge were also investigated. On overdischarge, a solvent decomposition plateau was observed in the discharge curves of Li/TiS_2 cells at < 1.1 V. The overdischarge resulted in a dendritic plating of lithium on subsequent recharges, leading to deterioration of cell performance. The residual current on constant-voltage overcharge for fresh and cycled Li/TiS_2 cells remained at 10–30 $\mu A\,cm^{-2}$ in the trickle-charge region of 2.5 V–3.0 V. On further increasing the charging voltage to > 3.25 V, the cell current reached the initially set limiting current, i.e., several $mA\,cm^{-2}$, due to the reaction $2(SCN)^- \rightarrow (SCN)_2 + 2e$ at the TiS_2 electrode, with lithium deposition occuring at the other electrode.

Upon completion of the cycling tests, the spent cells were taken apart in a nitrogen atmosphere and examined. A grey film, which contained trace Ti, S, C, as revealed by X-ray fluorescence spectra, was present on the anode. The lithium metal had been rendered porous. The microporous separator was covered with the metal on both sides. There

Table 2. TiS_2 (versus Li reference) half-cell investigation. TiS_2: 214 mA h, Li: 600 mA h, recharge: 5 mA

Cycle number	*Discharge* (% MU)	*Recharge* (% previous discharge)	*State-of-charge balance* (mA h)	*Discharge* (% state-of-charge)	*Discharge current* (mA)	*Cumulative capacity* (mA h)
1	89.6	81.6	179	89	10	191
2	73	96.9	174	87.4	10	348
5	69	98.7	166	87.8	10	797
10	66	98.8	160	87.8	10	1512
15	60	100	146	88.6	10	2196
20	52	100	135	82.9	10	2802
25	47	99	130	78.3	10	3226
26	52	100	130	86.9	5	3339
27	53	117*	139	86.6	5	3566
28	59	–	–	–	2.5	3691

Figure-of-merit†
$TiS_2 = 3691/214 = 17.3$
$Li = 3691/600 = 6.15$

Average efficiency

$$TiS_2 = \frac{3691}{3618 + 214} \times 100 = 96.3\%$$

$$Li = \frac{3691}{3618 + 600} \times 100 = 87.7\%$$

Cumulative rechargeable capacity
$(3691 - 2.7 \times 28) = 3618$ mA h

* Recharged to 2.8 V in the following sequence: 114.7 mA h at 5.0 mA, + 10.9 mA h at 1.0 mA, + 3.4 mA h at 0.50 mA, + 3.8 mA h at 0.25 mA. Total: 132.8 mA h on 27th cycle.

† Figure-of-merit $= \dfrac{\text{Cumulative discharge capacity in } N \text{ cycles}}{\text{Initial capacity of the electrode}}$.

was little or no free electrolyte in the cells. The 6.45 cm^2 area TiS_2 cathode exhibited softening to the extent of 2–5 mm from the periphery, with the remaining portion of the electrode being nearly of the same form as at the start of the cycling. The area of the softened portion was approximately 20–40% of the cathode.

In order to assess the effect of water, cells were assembled with electrolyte containing 1000 ppm of water. Although there was no noticeable immediate effect of water on cell performance, cells stored for one month at room temperature were inferior in that the TiS_2 material efficiency had dropped by > 80% to ~ 40% at the *C*/100 rate.

3. Discussion

3.1. *LiSCN–DOL–DME suitable for Li/TiS_2 cells*

The results that LiSCN is quite soluble in DOL and DOL–DME mixtures, including an extended liquid range to − 55° C, combined with solution resistivities of 200–400 Ω cm at room temperature, suggested that the electrolyte system is of interest for medium- and low-rate lithium cells. The lithium metal compatibility at 65° C and the voltage-scan results indicated that LiSCN–DOL–DME meets the chemical and electrochemical requirements for an organic electrolyte, secondary lithium cell in the voltage range for Li/TiS_2 cells.

3.2. *Scope of LiSCN–DOL–DME capability*

The primary discharge rate profile, shown in Figs. 3 and 4 for 10–45 mA h cm^{-2} cells, indicates that cells can be discharged at 1.5 mA cm^{-2} and deliver more than 60% of the theoretical capacity for 45% porous electrodes. The performance can be improved at room temperature by decreasing the charge density (Fig. 3 and Table 2, columns 1–4) and, at the same charge density, by increasing the temperature (Fig. 4). Li/TiS_2 cells operating at − 12° C deliver more than 80% MU at 1.6 mA (~ *C*/100 rate).

Li/TiS_2 cell recharge with LiSCN–DOL–DME to 2.8 V is not limited by electrochemical side reactions. However, the formation of oligomers, found in electrolyte studies, may interfere with electrode processes at higher rates. The cause of oligomerization of dioxolane may be the reaction of the solvent with $(SCN)_2$ formed by the interaction of peroxide impurities in the cyclic ether.

3.3. *Cell studies*

Table 1 gives the cycling results of Li/TiS_2 cells with charge capacity from 10–30 mA h cm^{-2}. The first discharges of the cells are noted to be higher for cells with lower charge density cathodes. However, no systematic cathode charge density trend is observed in cycle life to 30–40% MU. Thus, 30 mA h cm^{-2} cells with 3:1::Li:TiS_2 deliver ~ 10–20 cycles, and for ~ 15 mA h cm^{-2} cells, ~ 15 cycles are observed at 10 mA. Decreasing the discharge rate and increasing the Li/TiS_2 ratio increases the cycle life. Cells with 3:1::Li:TiS_2 ratio operate at ~ 20–40 cycles at *C*/20 and cells with 6:1::Li:TiS_2 operate at ~ 35–50 cycles at *C*/5–*C*/15 rate. Further, the cumulative capacity data and the low-rate test data in Table 1 suggest an equivalent of 40 deep-discharge cycles with an average efficiency of 70% MU at 1.6 mA (~ *C*/100) for ~ 25 mA h cm^{-2} TiS_2 cells at 23° C. This is an interpretation based on the expected accumulation of 700 mA h cm^{-2} in 40 cycles at an average efficiency of 70% MU for cells with 25 mA h cm^{-2} TiS_2 loading, which is approached in the test results in Table 2. It is seen that the average efficiency of lithium and TiS_2 electrodes exceeded 85% and 95%, respectively, from the data in Table 2. The TiS_2 half-cell operated between 89–78% MU, based on the state-of-charge, leading to an average loss of 0.1% charge capacity per cycle, as seen from Table 2, column 5.

3.4. *Causes of loss of capacity*

It was of interest to examine the cause of loss of output capacity from > 80% MU on first cycle to ~ 60% on the 40th cycle, as observed in the experiments. TiS_2 half-cell data in Table 2 indicate that there is a sharp drop in the state-of-charge of the TiS_2 electrode due to the lack of 100% recharge during the first few cycles with only 85% recharge on the first cycle. One factor contributing to this behaviour may be the loss of structural integrity of the cathode, noted in softening at the edges of cycled cathodes in the autopsy. This may have resulted from possible high-current-density operation at the edges.

Another factor contributing to the fading is related to the chemistry of the system. The formation of poly-DOL oligomers and the grey film on the anode, which contained products of reactions of impurities from the cathode (for example, sulphur and fine particles of TiS_2 transported across the separator) and water in the electrolyte are the leading pieces of evidence.

It is pointed out that in order to achieve deep-discharge cycling, a low cut-off potential of 1.2–1.4 V was employed, whereas the Li/TiS_2 open-circuit potential is 1.8 V [2]. All the factors discussed as possible causes of fading increase the cell *IR*. Intercalation of Na^+ ions leached from the fibreglass separator and co-intercalation of DME may also account for the suppression of cell voltage. In spite of the limitations, a typical cell (Table 2) offers an overall utilization of 96.3% for TiS_2 and 87.5% for lithium. Figures-of-merit of 28 and 7.8 obtained in ~ 40 cycles for TiS_2 and Li are approached or achieved in ~ 25–30 mA h cm^{-2} cells.

3.5. *Energy density and cost*

Based on the average cell voltage of 1.95 V and 70% material efficiency, the 25 mA h cm^{-2} cathode-limiting charge density of the as-yet unoptimized test cell was 0.14 W h cm^{-3}. The solute, based on SCN^-, is potentially a low-cost material, since ammonium thiocyanate is a by-product in scrubbing of volatile cyanide from coal gas with milk of sulphur in ammonium hydroxide. This low-cost feature, abundant availability and the vast literature on the chemistry of thiocyanates, render the thiocyanate salt an attractive candidate for lithium, organic electrolytes. Optimization of cathode structure, reduction of impurity levels and operating the system in a sealed-cell mode are indicated for further improving the Li/TiS_2 cell performance.

4. Safety note on handling the electrolyte

Thermal decomposition of LiSCN–DOL was studied with regard to safety aspects. The results showed that the decomposition of LiSCN to volatile cyanide is < 0.01 wt% in dry air, and 0.5–1.5 wt% in the presence of moist air and/or DOL at 650° C. Based on the results, caution is recommended in handling thermal run-away conditions.

Acknowledgement

The authors wish to acknowledge the assistance of M. T. Vidnansky, R. J. Solarczyk and R. W. Thomas in the experimental work.

References

[1] B. M. L. Rao, R. W. Francis and H. A. Christopher, *J. Electrochem. Soc.* **124** (1977) 1490.
[2] M. S. Whittingham, *Prog. Solid State Chem.* **12** (1978) 1.
[3] L. H. Gaines, R. W. Francis, G. H. Newman and B. M. L. Rao, *Proc. 11th IECEC* (1976).
[4] G. H. Newman and L. P. Klemann, *Electrochemical Society Fall Meeting*, Abstract 26, **79-2** (1979).
[5] G. L. Holleck, K. M. Abraham and S. B. Brummer, *Electrochemical Society Fall Meeting* Abstract 29, **79-2** (1979).
[6] D. A. Lee, *Inorg. Chem.* **3** (1964) 289.
[7] D. Saar, J. Brauner, H. Farber and S. Petrucci, *J. Phys. Chem.* **82** (1978) 545.
[8] V. R. Koch, US Patent 4 188 550 (1978).
[9] M. S. Whittingham, US Patent 4 009 052 (1977).
[10] M. L. Kronenberg, US Patent 3 951 685 (1976).
[11] B. H. Garth, US Patent 3 778 310 (1973).
[12] B. M. L. Rao, US Patent 4 002 492 (1977).
[13] R. F. Webb, A. J. Duke and L. S. Smith, *J. Chem. Soc.* (1962) 4307.